
Unifying Perspectives: Plausible Counterfactual Explanations on Global, Group-wise, and Local Levels

Patryk Wielopolski

Wrocław University of Science and Technology

patryk.wielopolski@pwr.edu.pl

Oleksii Furman

Wrocław University of Science and Technology

oleksii.furman@gmail.com

Jerzy Stefanowski

Poznań University of Technology

jerzy.stefanowski@cs.put.poznan.pl

Maciej Zieba

Wrocław University of Science and Technology

Tooploox Sp. z o.o.

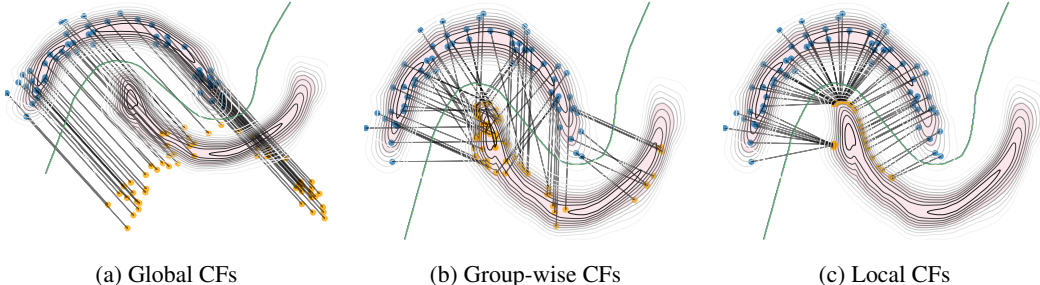
maciej.zieba@pwr.edu.pl

Abstract

Growing regulatory and societal pressures demand increased transparency in AI, particularly in understanding the decisions made by complex machine learning models. Counterfactual Explanations (CFs) have emerged as a promising technique within Explainable AI (xAI), offering insights into individual model predictions. However, to understand the systemic biases and disparate impacts of AI models, it is crucial to move beyond local CFs and embrace global explanations, which offer a holistic view across diverse scenarios and populations. Unfortunately, generating Global Counterfactual Explanations (GCEs) faces challenges in computational complexity, defining the scope of "global," and ensuring the explanations are both globally representative and locally plausible. We introduce a novel unified approach for generating Local, Group-wise, and Global Counterfactual Explanations for differentiable classification models via gradient-based optimization to address these challenges. This framework aims to bridge the gap between individual and systemic insights, enabling a deeper understanding of model decisions and their potential impact on diverse populations. Our approach further innovates by incorporating a probabilistic plausibility criterion, enhancing actionability and trustworthiness. By offering a cohesive solution to the optimization and plausibility challenges in GCEs, our work significantly advances the interpretability and accountability of AI models, marking a step forward in the pursuit of transparent AI.

1 Introduction

The increasing complexity and ubiquity of artificial intelligence (AI) systems in decision-making have intensified regulatory and societal demands for transparency (Goodman and Flaxman, 2017; Wachter et al., 2017). Explainable AI (XAI) addresses these demands by developing techniques to enhance the interpretability and understandability of AI models (Adadi and Berrada, 2018). It aims to elucidate the inner workings of complex models, enabling stakeholders to comprehend AI-driven decisions and assess their fairness and reliability (Samek and Müller, 2019). These methods are often categorized as global or local explanations. Global explanations provide a comprehensive understanding of



(a) Global CFs

(b) Group-wise CFs

(c) Local CFs

Figure 1: In this work, we introduce a unified approach for generating plausible local, group-wise, and global counterfactual explanations for differentiable classification models. The figure illustrates three types of explanations generated by our approach: (a) *global counterfactual explanations*, identifying a single direction of change applicable to the entire dataset; (b) *group-wise counterfactual explanations*, providing vectors of change for specific subgroups; and (c) *local counterfactual explanations*, offering instance-specific shift vectors, indicating minimal adjustments needed to alter predictions for individual cases.

the relationships between input features and output variables across the entire dataset, while local explanations focus on the reasons behind a model's prediction for a specific instance.

Counterfactual explanations (CFs) provide actionable insights into AI decision-making by illustrating how changes in input features of the observation can alter model predictions (Wachter et al., 2017). These "what-if" scenarios help users understand the relationships between inputs and outcomes, empowering them to make adjustments for desired results. For example, a CF might inform a loan applicant how to modify their application's attributes to qualify for a loan, offering more practical guidance than merely listing influential features. This actionable feedback is valuable across various fields; see (Guidotti, 2022; Stefanowski, 2023) for reviews.

In their classic formulation, Wachter et al. (2017) define CFs with two basic properties: validity (ensuring the achievement of the desired classification y') and proximity (minimizing the distance between the original instance \mathbf{x}_0 and its counterfactual \mathbf{x}'). While these are fundamental, several additional properties are often sought to enhance the usefulness of CFs. These include sparsity (modifying a minimal set of features), actionability (suggesting realistic and feasible changes), and plausibility (ensuring the counterfactual aligns with the underlying data distribution), among others.

However, traditional CFs are primarily *local explanations*, focused on understanding individual predictions. They do not address the broader implications of model behavior across diverse subgroups and scenarios. To overcome this limitation, research has shifted towards the development of global CFs (Ramamurthy et al., 2020; Plumb et al., 2020), which aim to quantify the model's overall impact.

Global Counterfactual Explanations (GCEs) and Group-wise Counterfactual Explanations (GWCEs) extend individual explanations to a broader scope, as illustrated in Figure 1. While Local CFs provide counterfactual vectors for individual instances, GCEs generate a single representative vector for the entire dataset, and GWCEs provide vectors for specific subgroups. GCEs and GWCEs offer a broader view of model behavior across diverse scenarios by generating representative counterfactuals for entire datasets or subgroups. For instance, a GCE can reveal that a loan approval model disproportionately denies applications from a specific demographic, highlighting model impacts on different groups even if individual CFs suggest otherwise.

However, generating effective GCEs and GWCEs poses significant challenges. The computational complexity of identifying representative counterfactuals in large datasets or numerous subgroups requires efficient algorithms and optimization techniques (Ley et al., 2023). Ensuring the plausibility and representativeness of GCEs is crucial, as unrealistic or unrepresentative explanations can erode trust and hinder actionable insights. Additionally, defining the "global" scope necessitates careful consideration of relevant subgroups (Gao et al., 2021). These challenges underscore the need for innovative methods to efficiently generate accurate, plausible, and representative GCEs and GWCEs, thus advancing fairer and more transparent AI systems.

To address the aforementioned challenges, we propose a novel unified framework for generating local, group-wise, and global counterfactual explanations for differentiable classification models. Our approach leverages gradient-based optimization, formulating counterfactual generation as an optimization task to efficiently explore the feature space for explanations at three levels of granularity. To ensure the generated counterfactuals are not only capable of altering the model’s prediction but also realistic and likely to occur in the real world, we incorporate a probabilistic plausibility criterion into our framework. This criterion is implemented through density estimation of the training data using normalizing flows (Rezende and Mohamed, 2015), thereby grounding the explanations in the data distribution and enhancing their actionable insights for users.

In summary, our key contributions are:

- A novel unified approach for generating counterfactual explanations at local, group-wise, and global levels for differentiable classification models, leveraging gradient-based optimization.
- The first framework that integrates group-wise counterfactual generation with a novel view on probabilistic plausibility constraints.
- An experimental evaluation demonstrating our approach’s performance, providing the effective balance between validity, distance, plausibility, and number of shifting vectors.

2 Related Works

Local Counterfactual Explanations Local Counterfactual Explanations (CFs), introduced by Wachter et al. (2017), identify minimal feature changes in an input instance leading to a desired prediction outcome. Early methods relied on heuristics, producing CFs not always realistic. Recent research, including Dhurandhar et al. (2018), Russell (2019), Kanamori et al. (2020), and Mothilal et al. (2020), has focused on sophisticated techniques like contrastive explanations, gradient-based approaches, linear programming, and generative models to improve CF quality (see Guidotti (2022) for a comprehensive review). Despite these advancements, concerns about plausibility and actionable nature persist (Keane et al., 2021).

Plausible Counterfactual Explanations The notion of plausibility in counterfactual explanations refers to the likelihood that suggested changes occur within the realistic subset of the training data manifold. Artelt and Hammer (2020) addressed this by introducing a probabilistic framework with density constraints to ensure counterfactuals have a high probability of belonging to the target class. Mahajan et al. (2019) emphasized preserving causal constraints to enhance plausibility and actionability. Poyiadzi et al. (2020) proposed incorporating a diversity constraint to generate diverse and plausible counterfactuals. Finally, Karimi et al. (2020) provided a comprehensive survey, highlighting related challenges and opportunities.

Global and Group-wise Counterfactual Explanations Definitions of Global Counterfactual Explanations (GCEs) and Group-wise Counterfactual Explanations (GWCEs) vary. Still, both aim to provide broader insights into model behavior, extending beyond individual predictions to groups of instances (GWCEs) or the entire dataset (GCEs). Early efforts like MAME (Ramamurthy et al., 2020) adapted local counterfactual techniques to create hierarchical explanation trees, showing feature importance at different levels of granularity. GIME (Gao et al., 2021) extended local methods to group contexts, optimizing fidelity and identifying Bayesian applicability regions for subgroups. Further, Plumb et al. (2020) used global translations in feature space to generate contrastive explanations between groups. AReS (Rawal and Lakkaraju, 2020; Ley et al., 2022) generated actionable rule sets for global model improvement, while GLOBE-CE (Ley et al., 2023) introduced scaling factors to GCEs and a scalable approach using random sampling and decision boundary approximation. Kanamori et al. (2022) proposed Counterfactual Explanation Trees (CET), utilizing decision trees to provide transparent and consistent actionable recourse by partitioning the input space and assigning actions based on the resulting structure.

In summary, while Global and Group-wise Counterfactual Explanations offer valuable insights, the field faces challenges like reliance on user-defined groups, limited generalizability, and ensuring plausibility of counterfactuals. Moreover, unifying local, group-wise, and global methods remain unresolved. Our work addresses these gaps by proposing a unified framework that generates plausible counterfactuals at all levels.

3 Background

Counterfactual Explanations Following Wachter et al. (2017), the local counterfactual explanations are defined as follows. Given a predictive model h and an initial input vector \mathbf{x}_0 within a d -dimensional real space \mathbb{R}^d , one seeks to determine a counterfactual instance \mathbf{x}' also in \mathbb{R}^d , where \mathbf{x}' is classified to desired class y' by the model h , $h(\mathbf{x}') = y'$. This is achieved through the optimization problem:

$$\arg \min_{\mathbf{x}' \in \mathbb{R}^d} d(\mathbf{x}_0, \mathbf{x}') + \lambda \cdot \ell(h(\mathbf{x}'), y'). \quad (1)$$

The function $\ell(\cdot, \cdot)$ refers to a loss function tailored for classification tasks such as the 0-1 loss or cross-entropy. On the other hand, $d(\cdot, \cdot)$ quantifies the distance between the original input \mathbf{x}_0 and its counterfactual counterpart \mathbf{x}' , employing metrics like the L1 (Manhattan) or L2 (Euclidean) distances to evaluate the deviation. The parameter $\lambda \geq 0$ plays a pivotal role in regulating the trade-off, ensuring that the counterfactual explanation remains sufficiently close to the original instance while altering the prediction outcome as intended.

Plausible Counterfactual Explanations The paper Artelt and Hammer (2020) extends the problem formulation of counterfactual explanations by adding a target-specific density constraint to enforce the plausibility of counterfactuals using a probabilistic framework. The optimization problem is formulated as follows:

$$\arg \min_{\mathbf{x}' \in \mathbb{R}^d} d(\mathbf{x}_0, \mathbf{x}') + \lambda \cdot \ell(h(\mathbf{x}'), y') \quad (2a)$$

$$\text{s.t. } \delta \leq p(\mathbf{x}'|y'), \quad (2b)$$

where $p(\mathbf{x}'|y')$ denotes conditional probability of the counterfactual explanation \mathbf{x}' under desired target class value y' and δ represents the density threshold.

Global and Group-wise Counterfactual Explanations In this work, we define Global Counterfactual Explanations (GCEs) as model instances generated by applying a single shift vector \mathbf{d} to the entire group of observations a user seeks to explain. In contrast, Group-wise Counterfactual Explanation (GWCE) methods aim to provide a single shift vector but within automatically identified subgroups of the dataset. GWCEs offer a more nuanced understanding of model behavior than a single GCE, especially in complex scenarios with non-linear decision boundaries (see Figure 1). By tailoring explanations to specific subgroups, GWCEs provide granular insights into the model's decision-making process, aiding in bias detection, mitigation, and performance improvement for specific populations. At the instance level, counterfactuals for both methods can be expressed as:

$$\mathbf{x}' = \mathbf{x}_0 + \mathbf{d}. \quad (3)$$

In contrast to the standard formulation, GLOBE-CE (Ley et al., 2023) introduces a scaling factor, k , specific to each observation, allowing for individual adjustments to the magnitude of the shift:

$$\mathbf{x}' = \mathbf{x}_0 + k \cdot \mathbf{d}. \quad (4)$$

4 Method

4.1 Global Counterfactual Explanations

The base problem of global counterfactual explanation assumes finding the global shifting vector \mathbf{d}^* . In order to solve that problem using optimization techniques, we can define the problem in the following way:

$$\arg \min_{\mathbf{d}} d^G(\mathbf{X}_0, \mathbf{X}') + \lambda \cdot \ell^G(h(\mathbf{X}'), y'), \quad (5)$$

where $\mathbf{X}_0 = [\mathbf{x}_{1,0}, \dots, \mathbf{x}_{N,0}]^T$ represents the matrix storing the initial input N examples, $\mathbf{X}' = [\mathbf{x}_{1,0} + \mathbf{d}, \dots, \mathbf{x}_{1,N} + \mathbf{d}]^T$ represent the extracted counterfactuals, after shifting the input examples with vector \mathbf{d} . Formally, $\mathbf{X}' = \mathbf{X}_0 + \mathbf{D}$, where $\mathbf{D} = \mathbf{1}_n \cdot \mathbf{d}^T$ and $\mathbf{1}_n$ represents N -dimesional

vector containing ones. We define a global distance as $d^G(\mathbf{X}_0, \mathbf{X}') = \sum_{n=1}^N d(\mathbf{x}_{n,0}, \mathbf{x}'_n)$, and global classification loss as an aggregation of the components: $\ell^G(h(\mathbf{X}'), y') = \sum_{n=1}^N \ell(h(\mathbf{x}'_n), y')$.

Extracting a single direction vector \mathbf{d} can be inefficient due to the dispersed initial positions \mathbf{X}_0 and, as discussed by Kanamori et al. (2022), it strictly depends on the farthest observation. Therefore, following the GLOBE-CE (Ley et al., 2023), we incorporate additional magnitude components and represent the counterfactuals as:

$$\mathbf{X}'_K = \mathbf{X}_0 + \mathbf{K}\mathbf{D}, \quad (6)$$

where \mathbf{K} is the diagonal matrix of magnitudes on the diagonal, i.e., $\mathbf{K} = \text{diag}(k_1, \dots, k_N)$. In order to ensure non-negative values of magnitudes, we represent them as $k_i = \exp(h_i)$. This formulation extends the classical vector-based update rule given by eq. (4) to the matrix notation. In order to extract the counterfactuals, we simply include \mathbf{X}_0 in eq. (5) and optimize \mathbf{K} together with \mathbf{d} .

4.2 Group-wise Counterfactual Explanations

Incorporating magnitude components into the global counterfactual problem enhances the shifting options during counterfactual calculation, yet the direction remains uniform across all observations. To address this, we propose a novel method that automatically identifies sub-groups represented by local shifting vectors with varying magnitudes. This approach restricts the number of desired shifting components to these identified subgroups. The formula for extracting group-wise counterfactuals is defined as:

$$\mathbf{X}'_{GW} = \mathbf{X}_0 + \mathbf{K}\mathbf{S}\mathbf{D}_{GW}, \quad (7)$$

where \mathbf{D}_{GW} is a matrix of size $K \times D$, K is the number of base shifting vectors and D is the dimensionality of the data. \mathbf{S} is a sparse selection matrix of size $N \times K$, where $s_{n,k} \in \{0, 1\}$ and $\sum_{k=1}^K s_{n,k} = 1$ for each of the considered rows. Practically, the operation selects one of the base shifting vectors \mathbf{d}_k , where $\mathbf{D} = [\mathbf{d}_1, \dots, \mathbf{d}_K]^T$, scaled by components k_n located on diagonal of matrix \mathbf{K} . Practically, we aim at optimizing the selection matrix \mathbf{S} together with base vectors \mathbf{D}_{GW} and magnitude components \mathbf{K} using the gradient-based approach. Optimizing binary \mathbf{S} directly is challenging due to the type of data and the given constraints. Therefore, we replace the \mathbf{S} with the probability matrix \mathbf{P} , where the rows $\mathbf{p}_{n,\bullet}$ represents the values of Sparsemax (Martins and Astudillo, 2016) activation function:

$$\mathbf{p}_{n,\bullet} = \arg \min_{\mathbf{p} \in \Delta} \|\mathbf{p} - \mathbf{b}_{n,\bullet}\|^2, \quad (8)$$

where $\Delta = \{\mathbf{p} \in \mathbb{R}^K : \mathbf{1}_K^T \mathbf{p} = 1, \mathbf{p} \geq \mathbf{0}_K\}$ and $\mathbf{b}_{n,\bullet}$ is n -th row of real-valued matrix \mathbf{B} . Practically, each row of the matrix \mathbf{P} represents a multinomial distribution, and matrix \mathbf{B} is optimized in the gradient-based framework.

The objective for extracting group-wise counterfactuals is as follows:

$$\arg \min_{\mathbf{K}, \mathbf{B}, \mathbf{D}_{GW}} d^G(\mathbf{X}_0, \mathbf{X}'_{GW}) + \lambda \cdot \ell^G(h(\mathbf{X}'_{GW}), y') + \lambda_s \cdot \ell_s(\mathbf{B}) + \lambda_k \cdot \ell_k(\mathbf{B}), \quad (9)$$

where $\ell_s(\mathbf{B})$ and $\ell_k(\mathbf{B})$ are entropy-based regularisers applied to preserve sparsity of matrix \mathbf{P} , and λ_s and λ_k are regularisation hyperparameters. The regularizer $\ell_s(\mathbf{B})$ is enforcing assignment to one group for each of the raw vectors $\mathbf{p}_{n,\bullet}$:

$$\ell_s(\mathbf{B}) = - \sum_{n=1}^N \sum_{k=1}^K p_{n,k} \cdot \log p_{n,k}. \quad (10)$$

The second regularisation component is responsible for reducing the number of groups extracted during counterfactual optimization:

$$\ell_k(\mathbf{B}) = - \sum_{k=1}^K p_k \cdot \log p_k, \quad (11)$$

where $p_k = \frac{\sum_{n=1}^N p_{k,n}}{\sum_{k=1}^K \sum_{n=1}^N p_{k,n}}$.

The problem formulation provided by eq. (7) and (9) represents the unified framework for counterfactual explanations. If the number of base shifting vectors in matrix \mathbf{D}_{GW} is equal to the number of examples ($K = N$), $\mathbf{S} = \mathbf{K} = \mathbb{I}$, and $\lambda_k = \lambda_s = 0$, the problem statements refer to standard formulation of local explanations. In the case where $\mathbf{D}_{GW} = \mathbf{D}$, $\mathbf{S} = \mathbf{K} = \mathbb{I}$, and $\lambda_s = \lambda_k = 0$, the statement pertains to standard global counterfactual explanations. When $\mathbf{K} \neq \mathbb{I}$, it is equivalent to the formulation given in Eq. 6, i.e., GCEs with magnitude. In other cases ($1 < K < N$), the problem is formulated as the group-wise explanation case. In this setting, we can disable automatic subgroup detection ($\lambda_k = 0$) and instead prioritize manual control over automatic number of subgroup formation ($\lambda_k > 0$). This latter configuration will be our primary focus for GWCEs.

The problem of extracting group-wise counterfactuals can also be executed in a two-stage procedure. In the first stage, the examples are clustered using a standard grouping method, i.e., K - means algorithm. In the second stage, the separate global counterfactual is extracted independently for each of the considered clusters. However, our end-to-end approach enables direct adjusting of the clusters together with a gradient-based counterfactual extraction procedure. Thus, no additional clustering is needed, optimizing the grouping for the best counterfactual explanations.

4.3 Plausible Counterfactual Explanations at All Levels

The plausibility is an important aspect of generating relevant counterfactuals. In this paper, we focus on density-based problem formulation, where the extracted example should satisfy the condition of preserving the density function value on a given threshold level (see eq. (2b)): $\delta \leq p(\mathbf{x}'|y')$. Moreover, we utilize a specific form of classification loss that enables better balancing between the plausibility and validity of the extracted examples.

The general criterion for extracting plausible group-wise counterfactuals can be formulated as follows:

$$\arg \min_{\mathbf{K}, \mathbf{B}, \mathbf{D}_{GW}} d^G(\mathbf{X}_0, \mathbf{X}'_{GW}) + \lambda \cdot (\ell^G(h(\mathbf{X}'_{GW}), y') + \ell_p(\mathbf{X}'_{GW}, y')) + \lambda_s \cdot \ell_s(\mathbf{B}) + \lambda_k \cdot \ell_k(\mathbf{B}), \quad (12)$$

where the loss component $\ell_p(\mathbf{X}'_{GW}, y')$ controls probabilistic plausibility constraint ($\delta \leq p(\mathbf{x}'|y')$) and is defined as:

$$\ell_p(\mathbf{X}'_{GW}, y') = \sum_{n=1}^N \max(\delta - p(\mathbf{x}'_{GW,n}|y'), 0), \quad (13)$$

where $\mathbf{x}'_{GW,n}$ is n -th counterfactual example stored in rows of $\mathbf{X}'_{GW} = [\mathbf{x}'_{GW,1}, \dots, \mathbf{x}'_{GW,N}]^T$ and δ is the density threshold defined by the user depending on the desired level of plausibility.

Various approaches, like Kernel Density Estimation (KDE) or Gaussian Mixture Model (GMM) can be used to model conditional density function $p(\mathbf{x}'_{GW,n}|y')$. In this work, we postulate the use of a conditional normalizing flow model (Rezende and Mohamed, 2015) to estimate the density. Compared to standard methods, like KDE or GMM, normalizing flows do not assume a particular parametrized form of density function and can be successively applied for high-dimensional data. Compared to other generative models, normalizing flows enables the calculation of density function directly using the change of variable formula and can be trained via direct negative log-likelihood (NLL) optimization. A detailed description of how to model and train normalizing flows is provided in the Supplement Material. Having the trained discriminative model $p_d(y'|\mathbf{x}'_{GW,n})$ and generative normalizing flow $p(\mathbf{x}'_{GW,n}|y')$ the set of counterfactuals \mathbf{X}'_{GW} is estimated using a standard gradient-based approach.

4.4 Validity Loss Component

The application of cross-entropy classification loss $\ell_p(\mathbf{X}'_{GW}, y')$ in eq. (12) constantly enforces 100% confidence of the discriminative model, which may have some negative impact on balancing other components in aggregated loss. In order to eliminate this limitation, we propose to replace $\ell^G(h(\mathbf{X}'_{GW}), y')$ with slightly different validity loss:

$$\ell_v(h(\mathbf{X}'_{GW}, y') = \sum_{n=1}^N \max \left(\max_{y \neq y'} p_d(y|\mathbf{x}'_{GW,n}) + \epsilon - p_d(y'|\mathbf{x}'_{GW,n}), 0 \right). \quad (14)$$

This guarantees that $p_d(y'|\mathbf{x}'_{GW,n})$ will be higher than the most probable class among the remaining classes by the ϵ margin. While using our criterion, the model can focus more on producing closer and more plausible counterfactuals.

5 Experiments

This study presents a comprehensive evaluation of our proposed counterfactual explanation method. Through qualitative and quantitative analyses, we assess its performance in local, group-wise, and global contexts. Additionally, we examine the impact of incorporating a plausibility criterion on the quality of generated explanations.

5.1 Experiments Details

Datasets and Classification Models We experimented with four numerical tabular datasets: *Law* and *Moons* (binary classification) and *Blobs* and *Wine* (multiclass classification). Details of these datasets are in the Supplement Material. We employed 5-fold cross-validation to assess model performance rigorously. The main manuscript reports mean performance across folds, while the Supplementary Material includes results with standard deviations. Our experiments use *Logistic Regression* and a 3-layer *Multilayer Perceptron* to evaluate both linear and nonlinear modeling. This combination ensures a robust assessment of model complexities, with both models being differentiable for our analytical methods.

Metrics In evaluating counterfactual explanations, we adopted a robust set of metrics mirroring those used by Guidotti et al. (2022). These metrics encompass: *Validity*, assessing the effectiveness of counterfactuals in altering the model’s decision; *Proximity*, quantified via *L1* and *L2* distances, indicating the closeness of counterfactuals to original instances; *Plausibility*, examined through *Local Outlier Factor (LOF)*, where values close to 1 denote normalcy and significantly higher values suggest outliers, and *Isolation Forest* scores, ranging from -0.5 to 0.5, with scores closer to -0.5 highlighting anomalies; *Probabilistic Plausibility (PP)*, denoting the proportion of counterfactuals meeting specific criteria; *Log Density*, assessing the likelihood of counterfactuals under the target class; and finally, *K*, measuring the number of vectors used to explain global counterfactuals.

Baselines For the baselines, we utilized various parameterizations of Eq. (7) as we cover counterfactual methods at all levels of granularity. Specifically, we employed *GCE* and *GCE w/ magnitude*, corresponding to the two cases detailed in Section 4.2. These can be interpreted as gradient-based adaptations of Plumb et al. (2020) and GLOBE-CE Ley et al. (2023). To provide a reference point and facilitate a more comprehensive comparison, we also included the Local CF (*LCF*) approach, as described in the aforementioned section. This method can be viewed as a gradient-based extension of the Wachter et al. (2017) approach. Furthermore, utilizing our proposed framework allows us to incorporate the plausibility criterion (*w/ PP*), a feature not present in previous methods.

5.2 Experiments Results

5.2.1 Qualitative Analysis

This section provides a detailed examination of the methods, focusing on two key aspects: the variation of resultant explanations across global, group-wise, and local contexts and the impact of the probabilistic plausibility criterion on the outcomes, as depicted in Figure 2. Initial observations (blue dots) and final counterfactual explanations (orange dots) cross the Logistic Regression decision boundary (green line) towards a probabilistically plausible region (red area) where the density meets plausibility thresholds.

For methods without the probabilistic plausibility criterion, we observe that all methods generate valid counterfactuals. The GCE method, however, produces outcomes significantly distant from the initial observations. Most methods provide a single change vector optimal for linear classifiers but

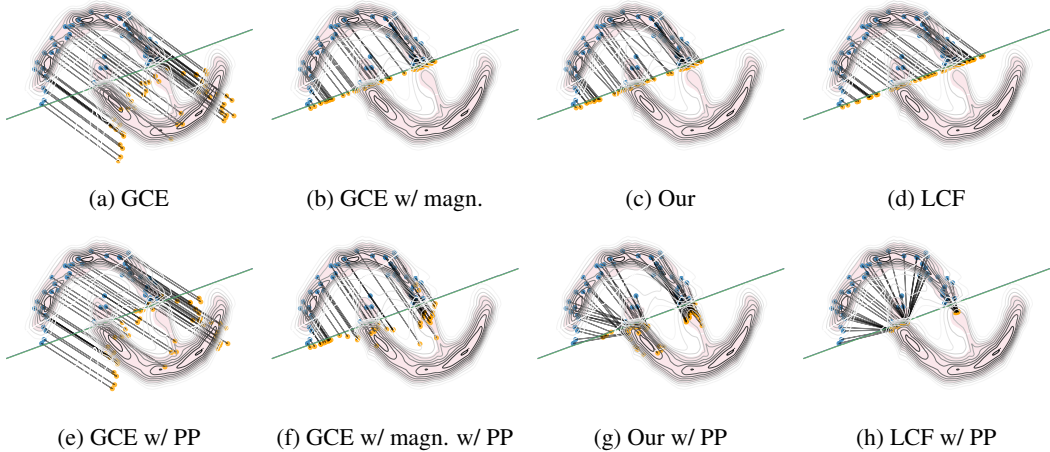


Figure 2: Illustration of the efficacy of various counterfactual explanation methods in traversing the decision boundary of a Logistic Regression model.

include many outlier observations. When the probabilistic plausibility criterion is applied, as shown in the second row of the figure, GCE methods struggle to generate valid counterfactuals and continue to produce outliers. Conversely, our approach and the LCF method show more promising results. Both generate valid counterfactuals, with our method effectively confining them within the desired density area, similar to LCF but with fewer shifting vectors.

In summary, incorporating probabilistic plausibility criteria yields outcomes that are less prone to outliers, potentially enhancing end-user usability. Moreover, within the framework of methods optimizing plausibility, we achieve results of comparable quality to the local counterfactual method, albeit with fewer shifting vectors.

5.2.2 Quantitative Analysis

In this section, we evaluate the efficacy of the global, group-wise, and local methods with the variant of our group-wise approach with probabilistic plausibility criteria. The results are summarized in Table 1, and extended results are presented in the Supplemental Material.

Firstly, all methods across all datasets and classification techniques achieved perfect or near-perfect validity results. For methods lacking the probabilistic plausibility criterion, the results often suggested outlier observations, as discussed in the previous section. When evaluating distance metrics, LCF consistently produced the best results, followed by our approach and GCE with magnitude, with GCE performing the least favorably. However, including probabilistic plausibility criteria in our approach significantly altered the performance landscape. Our approach with probabilistic plausibility almost always achieved plausible results while maintaining reasonable distances, often outperforming the GCE method. This demonstrates an effective trade-off, balancing plausibility and distance efficiently. Notably, this enhanced performance was achieved with a reasonable number of shifting vectors, underscoring the practicality of our method.

In conclusion, the evaluation demonstrates that all methods excel in validity, achieving near-perfect results. However, our group-wise approach integrating probabilistic plausibility criteria significantly enhances performance, consistently achieving plausible results while maintaining competitive distances with a low number of shifting vectors. This highlights an effective trade-off between plausibility and distance, showcasing the practicality and effectiveness of our method.

5.3 Limitations

An inherent limitation in our methodology arises from the reliance on gradient-based optimization techniques within the data space. This approach requires the use of differentiable discriminative models and, consequently, does not support categorical variables. Nonetheless, the landscape of contemporary modeling techniques largely mitigates this constraint, as many modern models are

Table 1: Comparison of counterfactual methods across different datasets for Logistic Regression and Multilayer Perceptron classification models.

DATASET	METHOD	K	VALIDITY \uparrow	PROB. PLAUS. \uparrow	LOG DENS. \uparrow	L1 \downarrow	L2 \downarrow
LOGISTIC REGRESSION							
BLOBS	GCE	1.00	1.00	0.36	0.14	0.66	0.49
	GCE w/ MAGN.	1.00	1.00	0.34	-0.66	0.53	0.39
	LCF	99.93	1.00	0.00	-2.17	0.45	0.32
	OUR	9.07	1.00	0.31	-1.08	0.52	0.38
	OUR w/ PP.	7.20	1.00	0.97	2.73	0.68	0.49
LAW	GCE	1.00	1.00	0.20	-1.41	0.90	0.58
	GCE w/ MAGN.	1.00	1.00	0.72	1.56	0.28	0.18
	LCF	222.00	1.00	0.78	1.80	0.36	0.21
	OUR	20.10	1.00	0.74	1.65	0.29	0.19
	OUR w/ PP.	31.10	1.00	0.98	2.05	0.44	0.27
MOONS	GCE	1.00	1.00	0.32	-8.97	0.72	0.53
	GCE w/ MAGN.	1.00	1.00	0.10	-0.17	0.36	0.27
	LCF	102.40	1.00	0.08	-1.26	0.42	0.30
	OUR	13.00	1.00	0.12	-0.09	0.37	0.28
	OUR w/ PP.	23.90	0.96	0.85	1.31	0.51	0.39
WINE	GCE	1.00	1.00	0.12	-2.23	1.98	0.61
	GCE w/ MAGN.	1.00	1.00	0.12	-0.82	1.49	0.44
	LCF	11.87	1.00	0.08	-2.14	1.49	0.42
	OUR	3.07	1.00	0.16	-1.44	1.72	0.50
	OUR w/ PP.	5.20	1.00	0.99	8.84	2.10	0.67
MULTILAYER PERCEPTRON							
BLOBS	GCE	1.00	1.00	0.41	1.45	0.62	0.44
	GCE w/ MAGN.	1.00	1.00	0.09	-0.42	0.49	0.35
	LCF	99.93	1.00	0.00	-2.54	0.41	0.29
	OUR	9.87	1.00	0.15	-0.01	0.51	0.37
	OUR w/ PP.	8.53	1.00	0.98	2.86	0.70	0.50
LAW	GCE	1.00	1.00	0.17	-5.07	1.08	0.65
	GCE w/ MAGN.	1.00	1.00	0.76	1.67	0.44	0.27
	LCF	238.60	1.00	0.84	1.96	0.46	0.27
	OUR	19.40	1.00	0.77	1.70	0.46	0.28
	OUR w/ PP.	37.40	0.95	0.98	2.17	0.47	0.29
MOONS	GCE	1.00	1.00	0.23	-99.19	0.82	0.66
	GCE w/ MAGN.	1.00	1.00	0.25	-27.20	0.53	0.45
	LCF	102.20	1.00	0.00	-1.82	0.26	0.20
	OUR	16.60	1.00	0.26	-7.27	0.46	0.35
	OUR w/ PP.	19.60	1.00	0.98	1.62	0.43	0.34
WINE	GCE	1.00	1.00	0.08	-1.67	2.01	0.63
	GCE w/ MAGN.	1.00	1.00	0.12	-1.39	1.52	0.46
	LCF	11.87	1.00	0.07	-3.18	1.59	0.45
	OUR	3.13	1.00	0.13	-2.03	1.76	0.52
	OUR w/ PP.	5.20	0.98	1.00	8.92	2.15	0.68

differentiable or can be adapted to include differentiable components. This integration capacity ensures that our method remains applicable across various settings.

6 Conclusions

In this work, we introduced a novel, unified framework for generating multi-level counterfactual explanations. This framework provides both granular and systemic insights into the behavior of differentiable classification models. By leveraging gradient-based optimization and incorporating probabilistic plausibility constraints, our method efficiently produces realistic individual, group-wise, and global explanations. Our experimental results demonstrate the effectiveness of this approach, generating plausible counterfactuals while maintaining competitive performance. This framework offers a valuable tool for practitioners and researchers seeking to enhance transparency, accountability, and trust in machine learning systems. By facilitating a more comprehensive understanding of model behavior across various levels of granularity, our method enables more informed decision-making and paves the way for future research in areas such as fairness analysis, model debugging, and decision support systems.

Broader Impact Our unified framework for multi-level counterfactual explanations has the potential to transform AI development by promoting transparency, fairness, and trust. By providing granular and systemic insights into model behavior, our approach empowers stakeholders to build more equitable and responsible AI systems across diverse domains. The group-wise analysis capabilities, particularly, offer a unique balance between interpretability and comprehensive understanding, ultimately leading to more informed decision-making and a broader societal impact.

References

Adadi, A. and Berrada, M. (2018). Peeking inside the black-box: A survey on explainable artificial intelligence (XAI). *IEEE Access*, 6:52138–52160.

Arteit, A. and Hammer, B. (2020). Convex density constraints for computing plausible counterfactual explanations. In *Artificial Neural Networks and Machine Learning - ICANN 2020 - 29th International Conference on Artificial Neural Networks, Bratislava, Slovakia, September 15-18, 2020, Proceedings, Part I*, volume 12396 of *Lecture Notes in Computer Science*, pages 353–365. Springer.

Dhurandhar, A., Chen, P., Luss, R., Tu, C., Ting, P., Shanmugam, K., and Das, P. (2018). Explanations based on the missing: Towards contrastive explanations with pertinent negatives. In *Advances in Neural Information Processing Systems 31: Annual Conference on Neural Information Processing Systems 2018, NeurIPS 2018, December 3-8, 2018, Montréal, Canada*, pages 590–601.

Dinh, L., Krueger, D., and Bengio, Y. (2015). NICE: non-linear independent components estimation. In *3rd International Conference on Learning Representations, ICLR 2015, San Diego, CA, USA, May 7-9, 2015, Workshop Track Proceedings*.

Dinh, L., Sohl-Dickstein, J., and Bengio, S. (2017). Density estimation using real NVP. In *5th International Conference on Learning Representations, ICLR 2017, Toulon, France, April 24-26, 2017, Conference Track Proceedings*.

Gao, J., Wang, X., Wang, Y., Yan, Y., and Xie, X. (2021). Learning groupwise explanations for black-box models. In *Proceedings of the Thirtieth International Joint Conference on Artificial Intelligence, IJCAI 2021, Virtual Event / Montreal, Canada, 19-27 August 2021*, pages 2396–2402. ijcai.org.

Goodman, B. and Flaxman, S. R. (2017). European union regulations on algorithmic decision-making and a "right to explanation". *AI Mag.*, 38(3):50–57.

Guidotti, R. (2022). Counterfactual explanations and how to find them: literature review and benchmarking. *Data Mining and Knowledge Discovery*, pages 1–55.

Kanamori, K., Takagi, T., Kobayashi, K., and Arimura, H. (2020). DACE: distribution-aware counterfactual explanation by mixed-integer linear optimization. In *Proceedings of the Twenty-Ninth International Joint Conference on Artificial Intelligence, IJCAI 2020*, pages 2855–2862. ijcai.org.

Kanamori, K., Takagi, T., Kobayashi, K., and Ike, Y. (2022). Counterfactual explanation trees: Transparent and consistent actionable recourse with decision trees. In *International Conference on Artificial Intelligence and Statistics, AISTATS 2022, 28-30 March 2022, Virtual Event*, volume 151 of *Proceedings of Machine Learning Research*, pages 1846–1870. PMLR.

Karimi, A., Barthe, G., Schölkopf, B., and Valera, I. (2020). A survey of algorithmic recourse: definitions, formulations, solutions, and prospects. *CoRR*, abs/2010.04050.

Keane, M. T., Kenny, E. M., Delaney, E., and Smyth, B. (2021). If only we had better counterfactual explanations: Five key deficits to rectify in the evaluation of counterfactual XAI techniques. In *Proceedings of the Thirtieth International Joint Conference on Artificial Intelligence, IJCAI 2021, Virtual Event / Montreal, Canada, 19-27 August 2021*.

Ley, D., Mishra, S., and Magazzeni, D. (2022). Global counterfactual explanations: Investigations, implementations and improvements. *CoRR*, abs/2204.06917.

Ley, D., Mishra, S., and Magazzeni, D. (2023). GLOBE-CE: A translation based approach for global counterfactual explanations. In Krause, A., Brunskill, E., Cho, K., Engelhardt, B., Sabato, S., and Scarlett, J., editors, *International Conference on Machine Learning, ICML 2023, 23-29 July 2023, Honolulu, Hawaii, USA*, volume 202 of *Proceedings of Machine Learning Research*, pages 19315–19342. PMLR.

Mahajan, D., Tan, C., and Sharma, A. (2019). Preserving causal constraints in counterfactual explanations for machine learning classifiers. *CoRR*, abs/1912.03277.

Martins, A. F. T. and Astudillo, R. F. (2016). From softmax to sparsemax: A sparse model of attention and multi-label classification. In *Proceedings of the 33nd International Conference on Machine Learning, ICML 2016, New York City, NY, USA, June 19-24, 2016*, volume 48 of *JMLR Workshop and Conference Proceedings*, pages 1614–1623. JMLR.org.

Mothilal, R. K., Sharma, A., and Tan, C. (2020). Explaining machine learning classifiers through diverse counterfactual explanations. In *FAT* '20: Conference on Fairness, Accountability, and Transparency, Barcelona, Spain, January 27-30, 2020*, pages 607–617. ACM.

Papamakarios, G., Murray, I., and Pavlakou, T. (2017). Masked autoregressive flow for density estimation. In *Advances in Neural Information Processing Systems 30: Annual Conference on Neural Information Processing Systems 2017, December 4-9, 2017, Long Beach, CA, USA*, pages 2338–2347.

Paszke, A., Gross, S., Massa, F., Lerer, A., Bradbury, J., Chanan, G., Killeen, T., Lin, Z., Gimelshein, N., Antiga, L., Desmaison, A., Kopf, A., Yang, E., DeVito, Z., Raison, M., Tejani, A., Chilamkurthy, S., Steiner, B., Fang, L., Bai, J., and Chintala, S. (2019). Pytorch: An imperative style, high-performance deep learning library. In *Advances in Neural Information Processing Systems 32*, pages 8024–8035. Curran Associates, Inc.

Plumb, G., Terhorst, J., Sankararaman, S., and Talwalkar, A. (2020). Explaining groups of points in low-dimensional representations. In *Proceedings of the 37th International Conference on Machine Learning, ICML 2020, 13-18 July 2020, Virtual Event*, volume 119 of *Proceedings of Machine Learning Research*, pages 7762–7771. PMLR.

Poyiadzi, R., Sokol, K., Santos-Rodríguez, R., Bie, T. D., and Flach, P. A. (2020). FACE: feasible and actionable counterfactual explanations. In *AIES '20: AAAI/ACM Conference on AI, Ethics, and Society, New York, NY, USA, February 7-8, 2020*, pages 344–350. ACM.

Ramamurthy, K. N., Vinzamuri, B., Zhang, Y., and Dhurandhar, A. (2020). Model agnostic multilevel explanations. In *Advances in Neural Information Processing Systems 33: Annual Conference on Neural Information Processing Systems 2020, NeurIPS 2020, December 6-12, 2020, virtual*.

Rawal, K. and Lakkaraju, H. (2020). Beyond individualized recourse: Interpretable and interactive summaries of actionable recourses. In Larochelle, H., Ranzato, M., Hadsell, R., Balcan, M., and Lin, H., editors, *Advances in Neural Information Processing Systems 33: Annual Conference on Neural Information Processing Systems 2020, NeurIPS 2020, December 6-12, 2020, virtual*.

Rezende, D. and Mohamed, S. (2015). Variational inference with normalizing flows. In *International Conference on Machine Learning*, pages 1530–1538. PMLR.

Russell, C. (2019). Efficient search for diverse coherent explanations. In *Proceedings of the Conference on Fairness, Accountability, and Transparency, FAT* 2019, Atlanta, GA, USA, January 29-31, 2019*, pages 20–28. ACM.

Samek, W. and Müller, K. (2019). Towards explainable artificial intelligence. In *Explainable AI: Interpreting, Explaining and Visualizing Deep Learning*, volume 11700 of *Lecture Notes in Computer Science*, pages 5–22. Springer.

Stefanowski, J. (2023). Multi-criteria approaches to explaining black box machine learning models. In *Asian Conference on Intelligent Information and Database Systems ACIIDS 2023*, pages 195–208. Springer.

Van Rossum, G. and Drake Jr, F. L. (1995). *Python reference manual*. Centrum voor Wiskunde en Informatica Amsterdam.

Wachter, S., Mittelstadt, B. D., and Russell, C. (2017). Counterfactual explanations without opening the black box: Automated decisions and the GDPR. *CoRR*, abs/1711.00399.

Table 2: The datasets utilized in our experiments are summarized below, detailing the number of samples (N), features (d), and classes (C) for each.

DATASET	N	d	C
BLOBS	1,500	2	3
LAW	2,220	3	2
MOONS	1,024	2	2
WINE	178	13	3

A Density Estimations using Normalizing Flows

Normalizing Flows have gained significant traction in generative modeling due to their flexibility and the straightforward training process through direct negative log-likelihood (NLL) optimization. This flexibility is rooted in the change-of-variable technique, which maps a latent variable \mathbf{z} with a known prior distribution $p(\mathbf{z})$ to an observed variable \mathbf{x} with an unknown distribution. This mapping is achieved through a series of invertible (parametric) functions: $\mathbf{x} = \mathbf{f}_K \circ \dots \circ \mathbf{f}_1(\mathbf{z}, y)$. Given a known prior $p(\mathbf{z})$ for \mathbf{z} , the conditional log-likelihood for \mathbf{x} is formulated as:

$$\log \hat{p}_F(\mathbf{x}|y) = \log p(\mathbf{z}) - \sum_{k=1}^K \log \left| \det \frac{\partial \mathbf{f}_k}{\partial \mathbf{z}_{k-1}} \right|, \quad (15)$$

where $\mathbf{z} = \mathbf{f}_1^{-1} \circ \dots \circ \mathbf{f}_K^{-1}(\mathbf{x}, y)$ is a result of the invertible mapping. The biggest challenge in normalizing flows is the choice of the invertible functions $\mathbf{f}_K, \dots, \mathbf{f}_1$. Several solutions have been proposed in the literature to address this issue with notable approaches, including NICE Dinh et al. (2015), RealNVP Dinh et al. (2017), and MAF Papamakarios et al. (2017).

For a given training set $\mathcal{D} = \{(\mathbf{x}_n, h(\mathbf{x}_n))\}_{n=1}^N$ we simply train the conditional normalizing flow by minimizing negative log-likelihood:

$$Q = - \sum_{n=1}^N \log \hat{p}_F(\mathbf{x}_n|y_n), \quad (16)$$

where $\log \log \hat{p}_F(\mathbf{x}_n|y_n)$ is defined by eq. (15). The model is trained using a gradient-based approach applied to the flow parameters stored in \mathbf{f}_k functions.

B Datasets

The details of the datasets are presented in Table 2. For preprocessing, we downsampled the majority class to address the class imbalance and normalized all features to the $[0, 1]$ range for consistency.

C Experiment Details

Hyperparameters For the regularization hyperparameters, we chose $\lambda = 1000$ and $\lambda_S = 1000$ and $\lambda_K = 100$, as these values demonstrated the most effective balance. More details are in the hyperparameter analysis section. Moreover, we selected the first quartile of the observed probabilities as our probability threshold δ .

Computational Resources In experiments, we used Python as the main programming language (Van Rossum and Drake Jr, 1995). Python with an open-source machine learning library PyTorch (Paszke et al., 2019) forms the backbone of our computational environment. We employed a batch-based gradient optimization method, which proved highly efficient by enabling the processing of complete test sets in a single batch. The experiments were executed on an M1 Apple Silicon CPU with 16GB of RAM, a configuration that provided enough computational power and speed to meet the demands of our algorithm.

D Hyperparameter Analysis

Analysis of influence of λ_K on number of created subgroups. We can observe in Tab. 3 that with the increase of λ_K number of subgroups decreases, meaning more clear explanations. However, it impacts (as expected) validity, probabilistic plausibility, and the distances in a negative way.

Table 3: Analysis of influence of λ_K on number of created subgroups.

λ_K	VALIDITY \uparrow	PROB. PLAUS. \uparrow	L1 \downarrow	L2 \downarrow	K
1	0.99	0.97	0.84	0.42	26.48
10	0.99	0.94	0.88	0.43	15.72
100	0.98	0.90	0.90	0.44	6.39
1000	0.97	0.85	0.91	0.44	2.50

Analysis of influence of λ_S on number of correctly assigned CF to group, i.e., exactly one subgroup was selected. Tab. 4 shows that with the increase of λ_S , number of correctly assigned CFs to relevant shifting vector increase, together with improvement with other metrics.

Table 4: Analysis of influence of λ_S on number of correctly assigned CF to group.

λ_S	VALIDITY \uparrow	PROB. PLAUS. \uparrow	L1 \downarrow	L2 \downarrow	CFs ASSIGNED TO GROUP \uparrow
1	0.98	0.91	0.90	0.44	0.95
10	0.98	0.91	0.89	0.44	0.97
100	0.98	0.91	0.87	0.43	0.99
1000	0.98	0.92	0.86	0.43	1.00

Analysis of influence of λ on validity, plausibility and distance. From Tab. 5, we can observe that with the increase of λ , validity and probabilistic plausibility metrics increase but in the cost of distance. It's an expected trade-off, as valid and plausible CFs usually lie farther away from the starting observation.

Table 5: Analysis of influence of λ on validity, plausibility and distance.

λ	VALIDITY \uparrow	PROB. PLAUS. \uparrow	L1 \downarrow	L2 \downarrow
1	0.97	0.82	0.77	0.39
10	0.98	0.90	0.81	0.40
100	0.99	0.95	0.91	0.44
1000	0.99	0.98	1.02	0.50

E Additional Experiments Results

In Table 6 and Table 7, we provide the experiment results for optimization with and without probabilistic plausibility criterion, respectively. The results are extended with standard deviations and additional metrics. Moreover, it's worth mentioning that calculation time depends on the method. The longest calculation time for global methods does not exceed 1 min. For our method, the longest calculation time for the whole dataset on one fold did not exceed 6 minutes on the resources mentioned above.

In Tables 6 and 7, we provide the experiment results for optimization with and without probabilistic plausibility criterion, respectively. The results are extended with standard deviations and additional metrics. Moreover, it's worth mentioning that calculation time depends on method. For global methods, the maximum average computation duration does not surpass 1 minute. In the case of the group-wise method, the maximum computation time required for processing the entire dataset across a single fold was under six minutes, utilizing the previously specified resources.

Table 6: Comparative Analysis of our method with other methods across various datasets and classification models. **Optimization with plausibility.**

DATASET	METHOD	K	VALID. \uparrow	PROB. PLAU.S. \uparrow	K SPARS. \uparrow	LOG DENS. \uparrow	L1 \downarrow	L2 \downarrow	ISOFOREST	LOF	TIME \downarrow
LOGISTIC REGRESSION											
BLOBS	GCE	1.0 \pm 0.0	1.0 \pm 0.0	0.76 \pm 0.04	1.0 \pm 0.0	2.60 \pm 0.08	0.74 \pm 0.15	0.53 \pm 0.11	0.02 \pm 0.01	1.09 \pm 0.01	21.95 \pm 4.29
	GCE w/ MAGN.	1.0 \pm 0.0	1.0 \pm 0.0	0.91 \pm 0.03	1.0 \pm 0.0	2.79 \pm 0.07	0.68 \pm 0.14	0.49 \pm 0.1	0.03 \pm 0.01	1.06 \pm 0.02	21.63 \pm 4.78
	LCF	99.93 \pm 0.59	1.0 \pm 0.0	1.0 \pm 0.0	1.0 \pm 0.0	2.29 \pm 0.05	0.59 \pm 0.15	0.43 \pm 0.11	0.01 \pm 0.01	1.10 \pm 0.04	12.11 \pm 2.18
	OUR	7.20 \pm 1.42	1.0 \pm 0.0	0.97 \pm 0.02	0.99 \pm 0.01	2.73 \pm 0.27	0.68 \pm 0.14	0.49 \pm 0.10	0.02 \pm 0.01	1.06 \pm 0.03	102.75 \pm 63.75
LAW	GCE	1.0 \pm 0.0	0.97 \pm 0.01	0.56 \pm 0.06	1.0 \pm 0.0	1.04 \pm 0.21	0.77 \pm 0.06	0.46 \pm 0.03	-0.0 \pm 0.01	1.11 \pm 0.02	17.53 \pm 5.92
	GCE w/ MAGN.	1.0 \pm 0.0	1.0 \pm 0.0	0.87 \pm 0.05	1.0 \pm 0.0	1.81 \pm 0.11	0.37 \pm 0.08	0.22 \pm 0.05	0.05 \pm 0.01	1.05 \pm 0.01	61.19 \pm 21.18
	LCF	222.0 \pm 11.92	1.0 \pm 0.0	1.0 \pm 0.0	1.0 \pm 0.0	1.88 \pm 0.11	0.35 \pm 0.02	0.21 \pm 0.01	0.06 \pm 0.01	1.03 \pm 0.0	20.0 \pm 9.67
	OUR	31.1 \pm 5.15	1.0 \pm 0.0	0.98 \pm 0.01	1.0 \pm 0.0	2.05 \pm 0.1	0.44 \pm 0.12	0.27 \pm 0.07	0.05 \pm 0.01	1.04 \pm 0.01	225.35 \pm 102.63
MOONS	GCE	1.0 \pm 0.0	0.91 \pm 0.06	0.34 \pm 0.06	1.0 \pm 0.0	-1.29 \pm 0.83	0.65 \pm 0.07	0.47 \pm 0.05	-0.01 \pm 0.01	1.40 \pm 0.10	45.23 \pm 17.94
	GCE w/ MAGN.	1.0 \pm 0.0	0.83 \pm 0.24	0.48 \pm 0.12	1.0 \pm 0.0	0.72 \pm 0.22	0.45 \pm 0.09	0.34 \pm 0.06	0.0 \pm 0.01	1.23 \pm 0.04	54.76 \pm 10.91
	LCF	102.4 \pm 3.75	1.0 \pm 0.0	0.99 \pm 0.03	1.0 \pm 0.0	1.26 \pm 0.07	0.46 \pm 0.07	0.35 \pm 0.04	0.03 \pm 0.01	1.0 \pm 0.03	63.31 \pm 15.34
	OUR	23.9 \pm 5.26	0.96 \pm 0.09	0.85 \pm 0.12	0.99 \pm 0.01	1.31 \pm 0.16	0.51 \pm 0.05	0.39 \pm 0.04	0.02 \pm 0.0	1.08 \pm 0.04	181.11 \pm 5.52
WINE	GCE	1.0 \pm 0.0	0.98 \pm 0.03	0.55 \pm 0.29	1.0 \pm 0.0	6.75 \pm 1.97	2.34 \pm 0.31	0.77 \pm 0.08	0.05 \pm 0.02	1.08 \pm 0.08	8.23 \pm 2.08
	GCE w/ MAGN.	1.0 \pm 0.0	1.0 \pm 0.0	0.63 \pm 0.28	1.0 \pm 0.0	7.43 \pm 1.79	2.16 \pm 0.31	0.72 \pm 0.09	0.06 \pm 0.02	1.07 \pm 0.07	7.53 \pm 4.06
	LCF	11.87 \pm 1.81	1.0 \pm 0.0	1.0 \pm 0.0	1.0 \pm 0.0	8.2 \pm 0.57	1.57 \pm 0.22	0.48 \pm 0.07	0.08 \pm 0.01	1.03 \pm 0.02	4.99 \pm 0.03
	OUR	5.20 \pm 1.32	1.0 \pm 0.0	0.99 \pm 0.03	0.98 \pm 0.05	8.84 \pm 0.48	2.1 \pm 0.36	0.67 \pm 0.11	0.07 \pm 0.01	1.04 \pm 0.03	21.15 \pm 5.66
MULTILAYER PERCEPTRON											
BLOBS	GCE	1.0 \pm 0.0	1.0 \pm 0.0	0.75 \pm 0.05	1.0 \pm 0.0	2.6 \pm 0.09	0.74 \pm 0.15	0.53 \pm 0.11	0.02 \pm 0.01	1.09 \pm 0.02	11.37 \pm 1.5
	GCE w/ MAGN.	1.0 \pm 0.0	1.0 \pm 0.0	0.91 \pm 0.03	1.0 \pm 0.0	2.78 \pm 0.08	0.68 \pm 0.14	0.49 \pm 0.1	0.03 \pm 0.01	1.06 \pm 0.02	11.41 \pm 5.41
	LCF	100.0 \pm 0.38	1.0 \pm 0.0	1.0 \pm 0.0	1.0 \pm 0.0	2.3 \pm 0.05	0.6 \pm 0.15	0.43 \pm 0.11	0.02 \pm 0.01	1.08 \pm 0.03	6.11 \pm 0.01
	OUR	8.53 \pm 1.88	1.0 \pm 0.01	0.98 \pm 0.03	1.0 \pm 0.01	2.86 \pm 0.20	0.70 \pm 0.14	0.5 \pm 0.11	0.03 \pm 0.01	1.05 \pm 0.02	84.15 \pm 80.8
LAW	GCE	1.0 \pm 0.0	0.90 \pm 0.02	0.62 \pm 0.03	1.0 \pm 0.0	0.95 \pm 0.27	0.67 \pm 0.02	0.41 \pm 0.01	-0.01 \pm 0.01	1.13 \pm 0.02	19.34 \pm 9.08
	GCE w/ MAGN.	1.0 \pm 0.0	0.93 \pm 0.05	0.81 \pm 0.01	1.0 \pm 0.0	1.78 \pm 0.19	0.50 \pm 0.09	0.3 \pm 0.06	0.03 \pm 0.01	1.08 \pm 0.02	61.24 \pm 28.93
	LCF	236.4 \pm 25.07	0.96 \pm 0.01	1.0 \pm 0.0	1.0 \pm 0.0	2.19 \pm 0.12	0.45 \pm 0.02	0.27 \pm 0.03	0.05 \pm 0.01	1.04 \pm 0.01	27.22 \pm 31.05
	OUR	37.40 \pm 5.03	0.95 \pm 0.01	0.98 \pm 0.02	0.99 \pm 0.01	2.17 \pm 0.07	0.47 \pm 0.03	0.29 \pm 0.02	0.05 \pm 0.0	1.04 \pm 0.0	357.13 \pm 46.87
MOONS	GCE	1.0 \pm 0.0	0.66 \pm 0.12	0.24 \pm 0.08	1.0 \pm 0.0	-2.87 \pm 1.7	0.51 \pm 0.15	0.39 \pm 0.09	-0.02 \pm 0.01	1.53 \pm 0.08	10.15 \pm 4.35
	GCE w/ MAGN.	1.0 \pm 0.0	0.79 \pm 0.07	0.71 \pm 0.09	1.0 \pm 0.0	0.53 \pm 0.78	0.55 \pm 0.08	0.41 \pm 0.06	-0.0 \pm 0.01	1.24 \pm 0.08	55.29 \pm 31.72
	LCF	102.5 \pm 0.85	1.0 \pm 0.01	1.0 \pm 0.0	1.0 \pm 0.0	1.38 \pm 0.03	0.33 \pm 0.01	0.26 \pm 0.01	0.02 \pm 0.0	1.02 \pm 0.02	9.71 \pm 3.61
	OUR	19.60 \pm 2.84	1.0 \pm 0.01	0.98 \pm 0.02	0.98 \pm 0.02	1.62 \pm 0.05	0.43 \pm 0.03	0.34 \pm 0.02	0.02 \pm 0.01	1.02 \pm 0.01	152.08 \pm 67.06
WINE	GCE	1.0 \pm 0.0	0.96 \pm 0.05	0.53 \pm 0.30	1.0 \pm 0.0	6.35 \pm 2.47	2.43 \pm 0.37	0.79 \pm 0.10	0.05 \pm 0.02	1.08 \pm 0.08	8.81 \pm 2.72
	GCE w/ MAGN.	1.0 \pm 0.0	0.99 \pm 0.03	0.66 \pm 0.29	1.0 \pm 0.0	7.38 \pm 1.99	2.19 \pm 0.29	0.73 \pm 0.09	0.06 \pm 0.02	1.07 \pm 0.06	11.53 \pm 7.12
	LCF	11.80 \pm 2.04	0.98 \pm 0.04	1.0 \pm 0.0	1.0 \pm 0.0	8.26 \pm 0.90	1.63 \pm 0.23	0.5 \pm 0.08	0.08 \pm 0.01	1.03 \pm 0.02	5.64 \pm 0.51
	OUR	5.20 \pm 2.08	0.98 \pm 0.04	1.0 \pm 0.0	1.0 \pm 0.02	8.92 \pm 0.88	2.15 \pm 0.28	0.68 \pm 0.1	0.07 \pm 0.01	1.04 \pm 0.03	22.9 \pm 12.32

Table 7: Comparative Analysis of our method with other methods across various datasets and classification models. **Optimization without plausibility.**

DATASET	METHOD	K	VALID.↑	PROB. PLAUS.↑	K SPARS.↑	LOG DENS.↑	L1↓	L2↓	ISOFOREST	LOF	TIME↓
LOGISTIC REGRESSION											
BLOBS	GCE	1.0 ± 0.0	1.0 ± 0.0	0.36 ± 0.28	1.0 ± 0.0	0.14 ± 2.65	0.66 ± 0.04	0.49 ± 0.04	-0.04 ± 0.05	1.58 ± 0.56	9.15 ± 1.01
	GCE w/ MAGN.	1.0 ± 0.0	1.0 ± 0.0	0.34 ± 0.28	1.0 ± 0.0	-0.66 ± 3.87	0.53 ± 0.02	0.39 ± 0.03	-0.04 ± 0.05	1.68 ± 0.76	6.85 ± 0.06
	LCF	99.93 ± 0.59	1.0 ± 0.0	0.0 ± 0.02	1.0 ± 0.0	-2.17 ± 4.66	0.45 ± 0.02	0.32 ± 0.02	-0.05 ± 0.04	1.83 ± 0.75	6.43 ± 0.21
	OUR	9.07 ± 1.1	1.0 ± 0.0	0.31 ± 0.24	1.0 ± 0.0	-1.08 ± 4.37	0.52 ± 0.02	0.38 ± 0.03	-0.04 ± 0.05	1.74 ± 0.83	87.95 ± 29.52
LAW	GCE	1.0 ± 0.0	1.0 ± 0.0	0.2 ± 0.08	1.0 ± 0.0	-1.41 ± 1.11	0.9 ± 0.07	0.58 ± 0.05	-0.06 ± 0.02	1.36 ± 0.1	46.42 ± 2.35
	GCE w/ MAGN.	1.0 ± 0.0	1.0 ± 0.0	0.72 ± 0.09	1.0 ± 0.0	1.56 ± 0.27	0.28 ± 0.01	0.18 ± 0.01	0.05 ± 0.01	1.05 ± 0.02	45.19 ± 1.39
	LCF	222.0 ± 11.92	1.0 ± 0.0	0.78 ± 0.05	1.0 ± 0.0	1.8 ± 0.14	0.36 ± 0.01	0.21 ± 0.01	0.05 ± 0.01	1.05 ± 0.01	15.79 ± 0.32
	OUR	20.1 ± 1.66	1.0 ± 0.0	0.74 ± 0.09	1.0 ± 0.0	1.65 ± 0.25	0.29 ± 0.01	0.19 ± 0.01	0.05 ± 0.01	1.05 ± 0.02	356.27 ± 27.77
MOONS	GCE	1.0 ± 0.0	1.0 ± 0.0	0.32 ± 0.03	1.0 ± 0.0	-8.97 ± 8.98	0.72 ± 0.04	0.53 ± 0.02	-0.02 ± 0.01	1.58 ± 0.17	27.35 ± 12.06
	GCE w/ MAGN.	1.0 ± 0.0	1.0 ± 0.0	0.1 ± 0.11	1.0 ± 0.0	-0.17 ± 0.36	0.36 ± 0.02	0.27 ± 0.01	0.01 ± 0.0	1.26 ± 0.04	31.74 ± 1.04
	LCF	102.4 ± 3.75	1.0 ± 0.0	0.08 ± 0.05	1.0 ± 0.0	-1.26 ± 0.5	0.42 ± 0.02	0.3 ± 0.01	0.0 ± 0.0	1.34 ± 0.04	12.35 ± 0.5
	OUR	13.0 ± 1.25	1.0 ± 0.0	0.12 ± 0.1	1.0 ± 0.0	-0.09 ± 0.33	0.37 ± 0.02	0.28 ± 0.01	0.01 ± 0.0	1.25 ± 0.04	93.59 ± 4.17
WINE	GCE	1.0 ± 0.0	1.0 ± 0.0	0.12 ± 0.15	1.0 ± 0.0	-2.23 ± 7.25	1.98 ± 0.37	0.61 ± 0.12	0.02 ± 0.02	1.16 ± 0.08	48.63 ± 8.52
	GCE w/ MAGN.	1.0 ± 0.0	1.0 ± 0.0	0.12 ± 0.13	1.0 ± 0.0	-0.82 ± 4.36	1.49 ± 0.28	0.44 ± 0.07	0.04 ± 0.01	1.13 ± 0.06	42.57 ± 1.35
	LCF	11.87 ± 1.81	1.0 ± 0.0	0.08 ± 0.12	1.0 ± 0.0	-2.14 ± 4.64	1.49 ± 0.22	0.42 ± 0.06	0.04 ± 0.01	1.13 ± 0.06	20.37 ± 1.47
	OUR	3.07 ± 0.59	1.0 ± 0.0	0.16 ± 0.18	1.0 ± 0.0	-1.44 ± 4.9	1.72 ± 0.2	0.5 ± 0.05	0.03 ± 0.01	1.14 ± 0.07	39.02 ± 7.59
MULTILAYER PERCEPTRON											
BLOBS	GCE	1.0 ± 0.0	1.0 ± 0.0	0.41 ± 0.15	1.0 ± 0.0	1.45 ± 0.69	0.62 ± 0.11	0.44 ± 0.08	-0.01 ± 0.02	1.27 ± 0.14	7.71 ± 0.6
	GCE w/ MAGN.	1.0 ± 0.0	1.0 ± 0.0	0.09 ± 0.08	1.0 ± 0.0	-0.42 ± 1.53	0.49 ± 0.09	0.35 ± 0.07	-0.04 ± 0.03	1.63 ± 0.4	7.55 ± 0.12
	LCF	99.93 ± 0.46	1.0 ± 0.0	0.0 ± 0.0	1.0 ± 0.0	-2.54 ± 1.84	0.41 ± 0.1	0.29 ± 0.07	-0.05 ± 0.02	1.98 ± 0.57	7.17 ± 0.06
	OUR	9.87 ± 1.46	1.0 ± 0.0	0.15 ± 0.14	1.0 ± 0.0	-0.01 ± 1.62	0.51 ± 0.08	0.37 ± 0.06	-0.04 ± 0.03	1.56 ± 0.39	54.33 ± 6.41
LAW	GCE	1.0 ± 0.0	1.0 ± 0.0	0.17 ± 0.08	1.0 ± 0.0	-5.07 ± 4.64	1.08 ± 0.07	0.65 ± 0.03	-0.09 ± 0.01	1.52 ± 0.07	40.93 ± 26.46
	GCE w/ MAGN.	1.0 ± 0.0	1.0 ± 0.0	0.76 ± 0.02	1.0 ± 0.0	1.67 ± 0.11	0.44 ± 0.04	0.27 ± 0.02	0.03 ± 0.01	1.09 ± 0.01	61.98 ± 1.41
	LCF	238.6 ± 25.05	1.0 ± 0.0	0.84 ± 0.02	1.0 ± 0.0	1.96 ± 0.09	0.46 ± 0.03	0.27 ± 0.02	0.05 ± 0.0	1.06 ± 0.01	25.83 ± 0.59
	OUR	19.4 ± 1.95	1.0 ± 0.0	0.77 ± 0.01	1.0 ± 0.0	1.7 ± 0.11	0.46 ± 0.02	0.28 ± 0.01	0.03 ± 0.0	1.09 ± 0.01	301.69 ± 50.1
MOONS	GCE	1.0 ± 0.0	1.0 ± 0.0	0.23 ± 0.04	1.0 ± 0.0	-99.19 ± 117.08	0.82 ± 0.17	0.66 ± 0.09	-0.08 ± 0.01	2.82 ± 0.18	8.79 ± 1.46
	GCE w/ MAGN.	1.0 ± 0.0	1.0 ± 0.0	0.25 ± 0.1	1.0 ± 0.0	-27.2 ± 28.91	0.53 ± 0.04	0.45 ± 0.04	-0.03 ± 0.01	1.89 ± 0.18	7.2 ± 0.32
	LCF	102.2 ± 0.45	1.0 ± 0.0	0.0 ± 0.0	1.0 ± 0.0	-1.82 ± 0.91	0.26 ± 0.01	0.2 ± 0.01	-0.0 ± 0.0	1.49 ± 0.09	6.85 ± 0.03
	OUR	16.6 ± 2.07	1.0 ± 0.0	0.26 ± 0.12	1.0 ± 0.0	-7.27 ± 11.31	0.46 ± 0.07	0.35 ± 0.06	-0.01 ± 0.01	1.51 ± 0.15	46.46 ± 36.72
WINE	GCE	1.0 ± 0.0	1.0 ± 0.0	0.08 ± 0.14	1.0 ± 0.0	-1.67 ± 5.35	2.01 ± 0.4	0.63 ± 0.13	0.02 ± 0.02	1.15 ± 0.07	54.21 ± 9.28
	GCE w/ MAGN.	1.0 ± 0.0	1.0 ± 0.0	0.12 ± 0.16	1.0 ± 0.0	-1.39 ± 5.37	1.52 ± 0.27	0.46 ± 0.07	0.04 ± 0.01	1.12 ± 0.06	42.5 ± 2.48
	LCF	11.87 ± 2.13	1.0 ± 0.0	0.07 ± 0.12	1.0 ± 0.0	-3.18 ± 8.09	1.59 ± 0.26	0.45 ± 0.07	0.04 ± 0.02	1.14 ± 0.07	21.88 ± 1.1
	OUR	3.13 ± 1.06	1.0 ± 0.0	0.13 ± 0.18	1.0 ± 0.0	-2.03 ± 8.46	1.76 ± 0.37	0.52 ± 0.09	0.04 ± 0.02	1.14 ± 0.07	34.31 ± 8.71